IL NUOVO CIMENTO **41 C** (2018) 224
DOI 10.1393/ncc/i2018-18224-3

COLLOQUIA: SIRR 2018

Ag X-ray fluorescence on different thickness and concentration layers

J. BROCCHIERI(1)(2)(*), E. SCIALLA(1)(2), F. AMBROSINO(1)(2), F. TERRASI(1)(2) and C. SABBARESE(1)(2)

(1) *Department of Mathematics and Physics, University of Campania "L. Vanvitelli" Caserta, Italy*
(2) *CIRCE, Center for Isotopic Research on the Cultural and Environmental heritage Viale Carlo III, 156, San Nicola La Strada (CE), Italy*

received 4 December 2018

Summary. — This work derives from the requirement to investigate on the silver surface enrichment of objects of historical and artistic interest using the X-ray fluorescence non-destructive technique (XRF). The aim is the thickness estimation through the experimental relationship between $\frac{K_\alpha}{K_\beta}$ and $\frac{K_\alpha}{L_\alpha}$ of Ag as a function of the thickness. Measurements on silver sheets of different thicknesses and three concentrations are carried out using a XRF spectrometer with a maximum voltage of 50 kV. The results allow to analyse the plating layer of silver objects also to make other interesting considerations.

1. – Introduction

The X-ray fluorescence technique (XRF) is a non-destructive spectroscopic technique widely used in the field of cultural heritage [1-3] for the qualitative and quantitative analysis of chemical elements. The X-ray fluorescence technique offers various advantages: it is non-destructive (so the integrity of the object is respected); the sample needs no preparation; it is really fast (it is possible to examine a large number of samples in a short time); it is relatively cheap; it is suitable for *in situ* measurements with portable equipment; the result of one measurement can be used for the qualitative and quantitative analysis of several elements. It uses primary X-rays that through their interaction with the matter produce fluorescence X-rays characteristic of the elements that make up a surface layer of the analysed sample. The knowledge of the depth distribution is

(*) Corresponding author. E-mail: jessica.brocchieri@unicampania.it

important to investigate the homogeneity of the sample and to point out the presence of layers of different materials. In the precious samples, in particular metal samples, a thin metal layer overlaps a metal sheet of another metal or alloy, *e.g.*, silver plating. However, surface measurements on ancient silver samples may not result in reliable bulk composition data due to silver enrichment of the near surface layer [4]. The composition and thickness of each layer may be determined. The detailed analysis of the fluorescence peaks and, in particular, of the relationships between the characteristic $\frac{K_\alpha}{K_\beta}$ and $\frac{K_\alpha}{L_\alpha}$ ratios of the same element, provides information that can also be used to estimate the thickness of the layer [5-10]. The functions that relate the values of these ratios to the layer thickness of the element in consideration are known theoretically by evaluating the absorption of incident and fluorescence photons in the material layer, but experimental evaluation is a useful application to verify and/or to extract characteristic parameters not easily estimated. The K/L ratio test was introduced [11] in order to assess the presence of a surface Ag-rich layer in ancient coins and to determine the thickness of this layer [12,13].

2. – Theoretical background

For a monoelemental sample the attenuation coefficient μ decreases with increasing energy and the thickness increases with increasing atomic number.

For any sample, self-attenuation effects must be considered and the trend of the ratios according to thickness is given by the self-absorption function [14]:

$$\frac{K_\alpha}{K_\beta} = \left(\frac{K_\alpha}{K_\beta}\right)_0 \cdot \frac{(\mu_0+\mu_2)}{(\mu_0+\mu_1)} \cdot \frac{1-e^{-(\mu_0+\mu_1)x}}{1-e^{-(\mu_0+\mu_2)x}}; \tag{1}$$

- $\left(\frac{K_\alpha}{K_\beta}\right)_0$ is the ratio of infinite thickness samples;
- μ_0 is the coefficient of linear attenuation of the element to the incident energy E_0 (cm^{-1});
- μ_1 is the coefficient of linear attenuation of the element to the energy of K_α line (cm^{-1});
- μ_2 is the coefficient of linear attenuation of the element to the energy of K_β line (cm^{-1});
- x is the sample thickness (cm).

The trend of the values of the ratio $\frac{K_\alpha}{L_\alpha}$ as a function of the thickness are described by eq. (1).

When the sample is constituted by an alloy, the attenuation coefficient of eq. (1) refers to the alloy concentration in this way:

$$\frac{K_\alpha}{K_\beta} = \left(\frac{K_\alpha}{K_\beta}\right)_0 \cdot \frac{(\mu_0+\mu_{12})c_1+(\mu_0+\mu_{22})c_2}{(\mu_0+\mu_{11})c_1+(\mu_0+\mu_{21})c_2} \cdot \frac{1-e^{-((\mu_0+\mu_{11})c_1+(\mu_0+\mu_{21})c_2))x)}}{1-e^{-((\mu_0+\mu_{12})c_1+(\mu_0+\mu_{22})c_2)x)}}; \tag{2}$$

- c_1 and c_2 are the concentrations of the elements 1 and 2 that make up the alloy and are such that $c_1+c_2=100\%$;
- $\left(\frac{K_\alpha}{K_\beta}\right)_0$ is the ratio of infinite thickness samples;

- μ_0 is the coefficient of linear attenuation of the element to the incident energy E_0 (cm^{-1});
- μ_{11} is the coefficient of linear attenuation of the element 1 to the energy of K_α line of 1 (cm^{-1});
- μ_{12} is the coefficient of linear attenuation of the element 2 to the energy of K_α line of 1 (cm^{-1});
- μ_{21} is the coefficient of linear attenuation of the element 1 to the energy of K_β line of 1 (cm^{-1});
- μ_{22} is the coefficient of linear attenuation of the element 2 to the energy of K_β line of 1 (cm^{-1});
- x is the sample thickness (cm).

3. – Materials and methods

Materials used for measurements are pure silver sheets, sheets of silver and copper of different thicknesses, sheets of Mylar, sheets of paper and silver samples, precisely:

- 7 sheets of 99.9% Ag having $2, 10, 14, 46, 90, 128, 223\,\mu$m thickness;
- 4 sheets of 92.9% Ag and 6.7% Cu having $52, 94, 152, 246\,\mu$m thickness;
- 4 sheets of 82.0% Ag and 17.9% Cu having $67, 94, 137, 198\,\mu$m thickness;
- 14 foils of Mylar having $23.8\,\mu$m thickness;
- 19 foils of commercial paper having $84\,\mu$m thickness;
- Plate, Pope Coin, 500 Lire coin, Dollar coin.

ED-XRF measurements are carried out using an instrument equipped by an X-ray tube with Rh anode (50 kV maximum dc voltage, $125\,\mu$A current, 2.5 W), a SSD detector having 160 eV energy resolution at 5.9 keV and $25\,\mathrm{mm}^2$ active area, an acquisition system and a spectral analysis software. The measurement time is 30 s and the investigated area is about $0.7\,\mathrm{cm}^2$. Spectra analysis is performed using a dedicated software to calculate Ag and Cu concentration and to extract the net area of K_α ($E = 22.16$ keV), K_β ($E = 24.94$ keV)and L_α ($E = 2.98$ keV) lines of X-rays fluorescence of Ag and K_α ($E = 8.05$ keV) and K_β ($E = 8.90$ keV) of Cu.

4. – Results

Two typical X-rays spectra coming from the interaction with a pure silver sheet (99%) and a sheet composed of silver and copper are displayed in fig. 1.

The net area values (or corresponding cps) of the K_α K_β and L_α Ag lines result variable with the sheet thickness and their trends are well fitted with growth curves having different slopes depending on different linear attenuation coefficients.

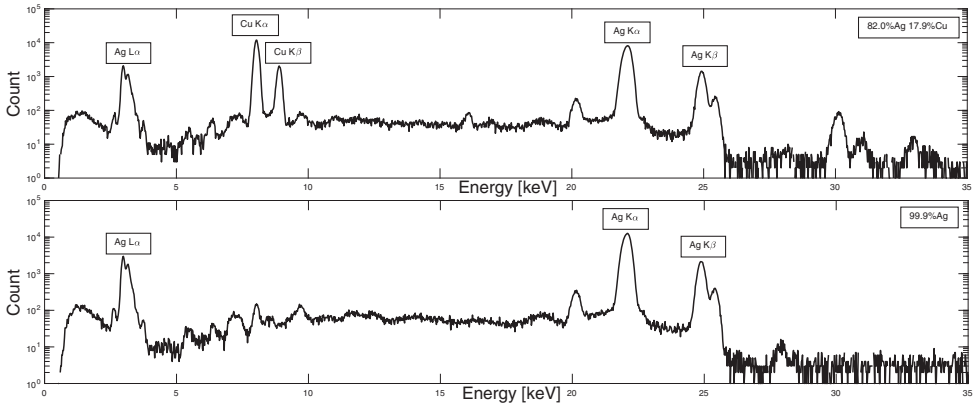

Fig. 1. – X-rays spectra coming from the silver samples.

The results of the measurements of different silver sheet thicknesses are useful to study the relation between the $\frac{K_\alpha}{K_\beta}$ ratio and the sheet thickness; in fig. 2 the $\frac{K_\alpha}{K_\beta}$ ratios of Ag *vs.* the Ag K_α count are reported for the three silver concentrations of the used sheets. The greater availability of data at the concentration of 99.9% of Ag allowed to obtain the complete trend showing that a low count corresponds to a thin thickness and the higher counts are due to the greater thicknesses. The trends at the concentrations of 92.9% and 82.9% were extrapolated from that at 99.9%. The values of the $\frac{K_\alpha}{K_\beta}$ ratio are little but significantly different for the thin sheets, and are much more different at thicknesses greater than 50 microns. The densification of points at higher counts is due to the self-absorption of the characteristic silver X-rays, which have been produced in the deepest part of the sheet.

To obtain a more sensitive method for evaluating the Ag thickness the $\frac{K_\alpha}{K_\beta}$ and $\frac{K_\alpha}{L_\alpha}$ ratios were calculated *vs.* sheet thickness at three different Ag concentrations; plots are displayed in figs. 3, 4 and 5.

Data are well fitted using the following equation, which contains the trend of both

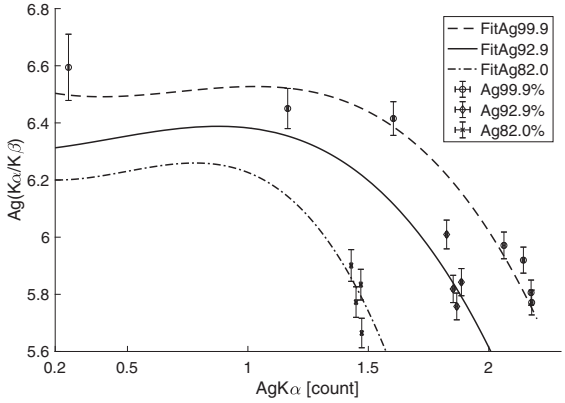

Fig. 2. – Ag K_α/K_β values *vs.* K_α count at three silver concentrations.

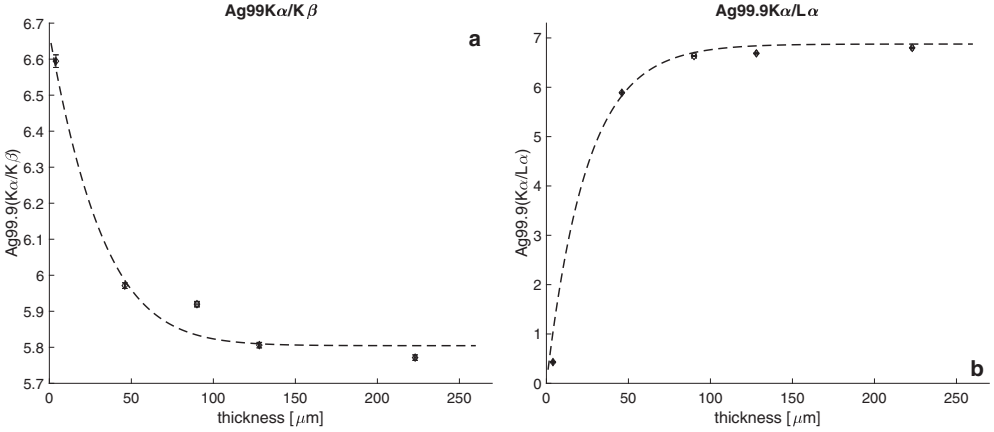

Fig. 3. – K_α/K_β and K_α/L_α ratios of Ag 99.9% *vs.* sheet thickness and fit curve using eq. (3).

the curves described by eq. (1) and eq. (2):

$$\frac{K_\alpha}{K_\beta} = a \cdot \frac{c}{b} \cdot \frac{1 - e^{-bx}}{1 - e^{-cx}}, \tag{3}$$

where

- $a = \left(\frac{K_\alpha}{K_\beta}\right)_0$ for both eq. (1) and eq. (2);
- $b = (\mu_0 + \mu_1)$ for eq. (1) and $b = (\mu_0 + \mu_{11})c_1 + (\mu_0 + \mu_{21})c_2$ for eq. (2);
- $c = (\mu_0 + \mu_2)$ for eq. (1) and $c = (\mu_0 + \mu_{12})c_1 + (\mu_0 + \mu_{22})c_2$ for eq. (2).

The results show that the trends of two ratios follow the theoretical trends. Fit coefficients and their uncertainties are reported in table I.

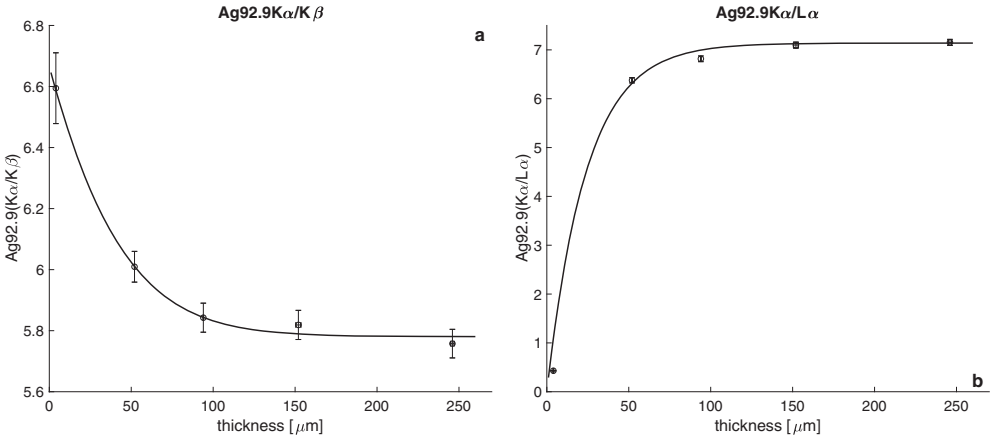

Fig. 4. – K_α/K_β and K_α/L_α ratios of Ag 92.9% *vs.* sheet thickness and fit curve using eq. (3).

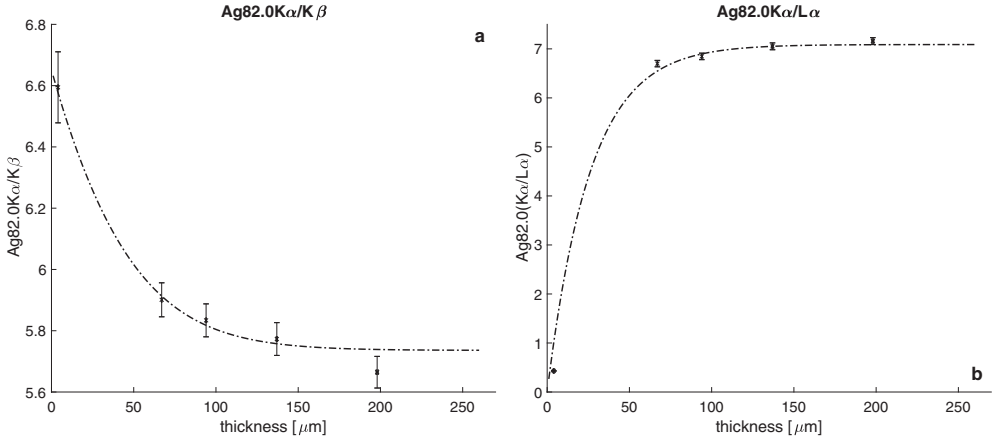

Fig. 5. – K_α/K_β and K_α/L_α ratios of Ag 82.0% *vs.* sheet thickness and fit curve using eq. (3).

Two trends are different because the K_α and L_α fluorescence radiations of silver come from different depths due to difference in the attenuation values at two relative energies $E(K_\alpha) = 22.16\,\text{keV}$ and $E(L_\alpha) = 2.98\,\text{keV}$.

The value of the linear attenuation coefficient, μ_0, in these measurements is not always easy to determine because it depends on the characteristics of the X-ray tube and on the beam constitution in the sample [8]. For this, we extracted the μ_0 value from both different fit coefficients coming from eq. (1) and eq. (2), assuming that μ_1 and μ_2 have constant values (table II). The two obtained results for μ_0 are consistent values at the same concentration and are decreasing with decreasing Ag concentration according to the reduction of the silver concentration in the sheet. The corresponding X-rays energy of the tube-sheet system, E_0, turns out to grow with the reduction of silver in the sheets.

To use and verify the results obtained in this work, measurements were made on silver or silver-plated objects to obtain the thickness of silver; it is estimated for each considered

Table I. – *Fit coefficients and their uncertainties.*

	a	b (μm^{-1})	c (μm^{-1})
Ag 99.9%	5.8 ± 0.1	0.06 ± 0.021	0.05 ± 0.02
Ag 92.9%	5.78 ± 0.03	0.045 ± 0.003	0.039 ± 0.004
Ag 82.0%	5.73 ± 0.08	0.04 ± 0.03	0.04 ± 0.02

Table II. – *Values of the linear attenuation coefficient μ_0, determined by eq.* (1) *and eq.* (2)*, and of the corresponding X-ray energies of the tube system.*

	μ_0 (μm^{-1}), eq. (1)	μ_0 (μm^{-1}), eq. (2)	E_0 (keV)
Ag 99.9%	0.043 ± 0.001	0.043 ± 0.001	29
Ag 92.9%	0.0302 ± 0.0002	0.0299 ± 0.0002	33
Ag 82.0%	0.027 ± 0.002	0.026 ± 0.002	34

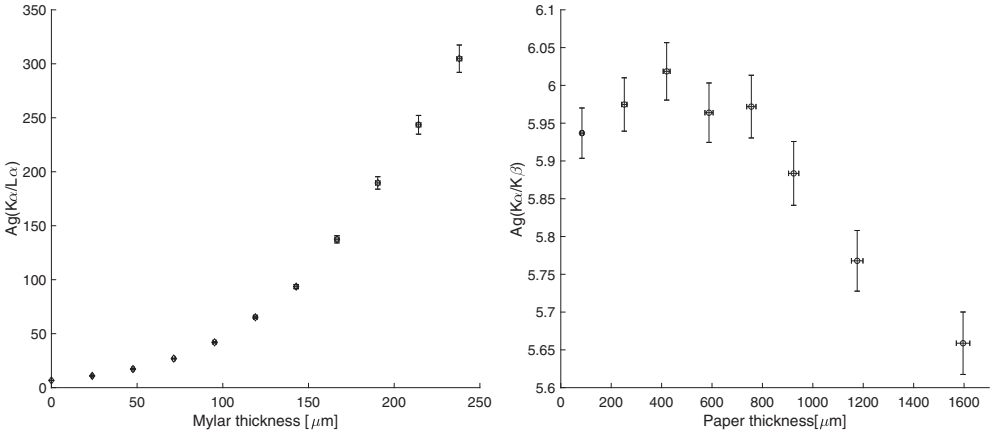

Fig. 6. – Ag $\frac{K_\alpha}{L_\alpha}$ values *vs.* Mylar thickness and Ag $\frac{K_\alpha}{K_\beta}$ *vs.* paper thickness.

object using the $\frac{K_\alpha}{K_\beta}$ ratio values (table III). The results are in good agreement within the measurement uncertainties with the already known values of those objects.

Using the Ag 99.9% thicker sheet, measurements were also carried out to study the attenuation of the Ag fluorescence lines through sheets of Mylar and commercial paper that contain no silver. When the Mylar covers the silver, the trend of the Ag $\frac{K_\alpha}{L_\alpha}$ ratio well describes the effect of the thickness increase so that the thickness of the Mylar could be obtained from it (fig. 6). Using commercial paper, the Ag $\frac{K_\alpha}{K_\beta}$ ratio values are significantly decreasing after 400 microns of paper thickness; also in this case from the graph of fig. 6 the thickness of the paper can be deduced.

5. – Conclusion

A systematic determination of the Ag $\frac{K_\alpha}{K_\beta}$ and Ag $\frac{K_\alpha}{L_\alpha}$ ratios was performed for different thicknesses of silver sheets and for three silver concentrations. The trends of these ratios as a function of the thickness of the Ag layer have been obtained and the concentrations of Ag have been approximated with the curves provided by the theory. Using the obtained trends, thicknesses of silver covering layers were estimated in some objects as a verification test of the results. The effect of absorption of the characteristic lines of Ag has also been studied through layers of Mylar and commercial paper.

TABLE III. – *Ag* $\frac{K_\alpha}{K_\beta}$ *values of some silver-plated objects and silver thickness obtained by the relative fit curve.*

Sample	K_α/K_β	thickness (μm)
Plate	5.98 ± 0.09	47 ± 2
Pope	6.5 ± 0.9	7 ± 1
500 Lire	5.85 ± 0.07	80 ± 5
Dollar	5.79 ± 0.08	> 160

REFERENCES

[1] Mantler M. and Schreiner M., *X-Ray Spectrom.*, **29** (2000) 3.
[2] Janssens K. *et al.*, *Top. Curr. Chem.*, **374** (2016) 81.
[3] Shugar A. N., *Portable X-ray Fluorescence and Archaeology: Limitations of the Instrument and Suggested Methods To Achieve Desired Results*, in *Archaeological Chemistry VIII*, edited by Armitage R. A. and Burton J. H., Vol. **1147** (ACS) 2013, Chapt. 10, pp. 173–193.
[4] Kantarelou V. *et al.*, *Spectrochim. Acta B*, **66** (2011) 681.
[5] Trojek T. *et al.*, *Appl. Radiat. Isot.*, **68** (2010) 871.
[6] Ferretti M. *et al.*, *Spectrochim. Acta B*, **83** (2013) 21.
[7] Cesareo R. *et al.*, *Nucl. Instrum. Methods B*, **267** (2009) 2890.
[8] Cesareo R. *et al.*, *Nucl. Instrum. Methods B*, **312** (2013) 15.
[9] Cesareo R., *Riv. Nuovo Cimento*, **23** (2000) 1.
[10] Linke R. *et al.*, *X-Ray Spectrom.*, **32** (2003) 373.
[11] Giancocelli A. *et al.*, *Appl. Phys. A* , **89** (2007) 92.
[12] Klockenkamper R. *et al.*, *Archaeometry*, **41** (2007) 311.
[13] Asderaki E. and Rehren T., in *Proceedings of the 34th International Symposium on Archaeometry, Zaragoza, Spain*, edited by Perez-Arontegui J. (Institución Fernando el Católico) 2004, p. 131.
[14] Cesareo R. *et al.*, *X-Ray Spectrom.*, **37** (2008) 309.